

Molecular Influences on Miscibility Patterns in Random Copolymer/Homopolymer Binary Blends

Jacek Dudowicz* and Karl F. Freed

The James Franck Institute and the Department of Chemistry, University of Chicago, Chicago, Illinois 60637

Received September 9, 1997; Revised Manuscript Received April 14, 1998

ABSTRACT: The lattice cluster theory (LCT) is used to study the microscopic molecular factors affecting the miscibilities of A_xB_{1-x}/C binary mixtures (where the homopolymer C is either different or identical to the A_xB_{1-x} random copolymer species). A prime goal of this study lies in describing gross departures of LCT predictions from the prevailing random copolymer Flory–Huggins (FH) theory. These departures are illustrated by analyzing computed constant pressure spinodal (and binodal) curves, and some computations are compared with experimental data. Different miscibilities are predicted for several A_xB_{1-x}/A and A_xB_{1-x}/B systems with $x = 1/2$, departing considerably from predictions of FH random copolymer theory. These differences are partially explained in terms of the entropic structural parameter that provides one measure of blend structural asymmetry. The computed phase diagrams of $A_xB_{1-x}/C \neq A, B$ blends exhibit richer miscibility patterns than those derived from FH random copolymer theory. The illustrations focus on the influence of monomer structure, interaction energies, and pressure on the phase behavior of random copolymer/homopolymer systems. Applications to polyolefins employ a model for interaction energies based on Lennard-Jones parameters for these olefins.

I. Introduction

Experimental and theoretical studies of random copolymers are driven by their considerable technological importance¹ and by their intrinsic scientific interest. The earliest theoretical descriptions^{2–4} of these systems are based on an extension^{5,6} to random copolymers of Flory–Huggins (FH) theory, which is widely used, in part, mainly because of its extreme simplicity. The random copolymer FH theory has been enormously successful in explaining the ability of random copolymers to enhance the compatibility of otherwise immiscible systems. On the other hand, this simple theory^{5,6} displays a complete insensitivity of the predicted thermodynamic properties to the monomer sequence, molecular architectures, monomer structures, and applied pressure. While the last deficiency can be eliminated by including⁷ blend compressibility into FH type models, the other severe limitations still remain and stem from the intrinsic assumptions of FH theories which represent all monomers as structureless entities.

The inability of FH theories to distinguish between different polymer structures arises, in part, because the theories omit a description of the short range correlations that are directly responsible for nonrandom mixing effects. For instance, FH type theories^{5,6} describe random copolymers, alternating copolymers, and diblock copolymers with the same monomer compositions as strictly identical systems. On the other hand, experiments evidence their different thermodynamic behaviors. For example, Winey *et al.*⁸ observe that pure PMMA is more miscible with the alternating PS-*co*-PMMA copolymer than with the symmetric random PS-*co*-PMMA copolymer. A similar preference in miscibilities has been noticed by Lohse *et al.*⁹ for polypropylene/ethylene-*co*-propylene mixtures, where the diblock is found to be the least miscible, the alternating copolymer is found to be the most miscible, and the statistical copolymer displays an intermediate miscibility. Recent molecular dynamics and molecular mechanics simula-

tions by Yao *et al.*¹⁰ also confirm the dependence of the interacting strength (miscibility) on the monomer sequence.

As a partial remedy for these deficiencies of random copolymer FH theories, several treatments^{11–13} postulate an *ad hoc* dependence of the system's free energy on the monomer sequence by introducing a set of phenomenological six (or four) monomer interaction parameters $\chi_{ijk,lmn}$ (or $\chi_{ij,kl}$) and by invoking additional assumptions to reduce the huge number of resultant $\chi_{ijk,lmn}$ parameters to a few. The use of a six-body interaction parameter, however, departs significantly from customary statistical mechanical descriptions based on pairwise additive nonbonded interactions.

The Bates–Fredrickson model¹⁴ of polyolefin blend miscibilities (driven solely by differences in the chain stiffness of the two blend species) is readily extended to random copolymers by using experimental data for the copolymer radii of gyration. However, the analysis of Graessley, Lohse, and co-workers^{15–17} indicates that a superior representation of the polyolefin miscibilities emerges from a solubility parameter model based on cohesive energies, quite the opposite limit of the Bates–Fredrickson approach. The more microscopic PRISM treatment^{18,19} emphasizes the combined influences of stiffness disparities and energetic interactions, while lattice cluster theory (LCT) computations^{20,21} illustrate the additional importance of differences in monomer molecular structures. Thus, we do not pursue detailed comparison with the Bates–Fredrickson model as applied to random copolymer systems.

A limitation of the solubility parameter model¹⁵ lies in its inability to explain many significant examples^{16,22} of nonrandom mixing behavior. One particular illustration of the latter is the observed¹⁶ better miscibility of head-to-head poly(propylene) than that of atactic poly(propylene) with poly(ethylene propylene), a difference whose molecular mechanism has recently been elucidated²³ with the aid of the LCT. Another limitation of

the solubility parameter model emerges, for instance, from the analysis of SANS data¹⁷ for hydrogenated poly-(butadienes) with randomness induced by varying degrees of 1,2 and 1,4 content. The solubility parameter model employs¹⁷ a separate set of temperature dependent solubility parameters for each system with differing amounts of 1,2 and 1,4 units. A more molecular model²⁴ replaces the plethora of solubility parameters by three monomer–monomer interaction energies or, better still, by united atom group CH_n ($n = 1, 2, 3$) interaction energies.

PRISM computations^{18,19} for random copolymers have to date only treated the copolymers as homopolymers with averaged monomers, an approach that cannot address the dependence of polymer properties on monomer sequence.

The lattice cluster theory^{25–27} (LCT) is free from all the above mentioned deficiencies. While a compressible extension⁷ of FH mean field theory plays the role of the zeroth order approximation, the underlying extended lattice model of the LCT allows²⁷ different monomers to occupy different numbers of lattice sites with connectivities chosen to mirror the relative monomer shapes and sizes. Nonrandom mixing effects are included in the LCT by appending corrections to the FH free energy that describe the local correlations induced by packing constraints and the different monomer–monomer interactions.²⁸ A monomer sequence dependence of the LCT free energy then emerges naturally from treating these correlation contributions in a perturbative fashion.²⁶ No assumptions are required concerning the particular form of the interaction parameters χ , and no new adjustable parameters appear for random copolymers beyond those already present in the LCT for the corresponding homopolymer blends.²⁶

The derivation of this more molecular oriented LCT description of random copolymer systems, however, involves enormous algebraic complexity,²⁶ especially when the individual A and B monomers of the random copolymer are permitted to have arbitrary molecular structures. In order to simplify the algebra and to avoid a proliferation of new counting indices, related statistical weights, averages, and so forth, the current version of the LCT has been derived²⁹ for models of random copolymers in which all monomers contain side groups and have vinyl structures with no tetrafunctional backbone units. Thus, this restriction presently precludes direct quantitative comparisons with experimental data for systems containing, for example, polyethylene or 1,4 addition polybutadiene and polyisoprene. However, some general qualitative behaviors of blends containing these polymers can be deduced (when interaction energies are not too disparate) from the strong correlation between the LCT entropic structural parameter and computed polyolefin blend miscibilities.^{20,21} Thus, in spite of the above limitations, the present random copolymer LCT can be applied to important systems, while a simplified version²⁴ is free of restrictions concerning monomer structures.

The present paper represents a continuation of our previous theoretical studies⁷ of a compressible generalization of FH random copolymer theory for predicting the miscibilities of $A_xB_{1-x}/C = A, B$ and A_xB_{1-x}/A_yB_{1-y} binary mixtures. The previous work focuses⁷ primarily on how compressibility (pressure) affects predictions of random copolymer FH theory and of how a LCT model for the entropic χ parameter can be used to extend the

theory to random copolymer systems displaying lower critical solution temperature (LCST) phase diagrams. The present work applies the general LCT to describe two classes of A_xB_{1-x}/C random copolymer/homopolymer blends. The first class involves systems with the homopolymer C identical to one of the copolymer species, while the second group contains mixtures where both copolymer and homopolymer species are different ($C \neq A, B$). The former blends have been investigated experimentally by Russell *et al.*³⁰ and Winey *et al.*,⁸ who report very different miscibilities for the symmetric random copolymer $\text{PS}_{0.5}\text{PMMA}_{0.5}$ with PS or PMMA. Standard FH theory predicts^{5,6} identical compatibilities for these two systems, while the extension of random copolymer FH theory to compressible systems produces⁷ only slight departures from this classic prediction. Unfortunately, the sequence dependence in copolymers with such large bulky side groups emerges from longer range correlations than those presently included in the LCT. Hence, we cannot explain the behavior of these systems until higher order LCT contributions have been evaluated.

The LCT analysis is also applied to LCST mixtures and to polyolefin blends whose computed phase boundaries exhibit both upper and lower critical temperatures. In a first attempt to approach the “ultimate” microscopic lattice model, the treatment of polyolefin systems is based on modeling the united atom group interactions by using Lennard-Jones (LJ) well depths^{31–34} e_{ij} taken from extensive off-lattice simulations for alkanes and polyolefins. The Berthelot geometrical mean combining rule is commonly employed^{31–34} for evaluating the hetrocontact LJ interaction parameters e_{ij} , and this combining rule persists for the monomer-averaged LCT energies ϵ_{ij} . As explained below, the Berthelot approximation appears suspect, especially for treating binary polyolefin homopolymer blends with net attractive exchange energies. This deficiency of the simple interaction model implies that the model is only suitable for probing general qualitative trends. Hence, a prime focus is placed on elucidating gross departures of LCT predictions from the prevailing theory of random copolymers, namely, that based on Flory–Huggins theory.

The second group of systems, considered with the LCT, involves binary blends of A_xB_{1-x} random copolymers and a homopolymer C of a distinct polymer species. Among many model A_xB_{1-x}/C polyolefin blends having vinyl A, B, and C monomers, we select those which display for a given random copolymer composition x a nearly vanishing FH interaction parameter χ_{FH} . An example with a negative χ_{FH} would provide an interesting illustration of these LCT computations, but the aforementioned interaction model does not produce $\chi_{\text{FH}} < 0$, probably again because of the use of the Berthelot geometrical mean rule. Standard FH theory would predict that a system with $\chi_{\text{FH}} = 0$ is completely miscible, while the LCT contrasts this simple picture with a rich array of miscibility patterns. This richness of the LCT predictions arises from the combined effects of monomer structures, nonrandom mixing, compressibility, and the monomer sequence dependence²⁶ of the LCT free energy.

Section I describes the extended lattice model for general A_xB_{1-x}/C random copolymer/homopolymer blends, reviews the basic features of the lattice cluster theory, and defines the interaction model for A_xB_{1-x}/C polyolefin systems. Illustrations of extensive LCT computations

for the spinodal curves (and some binodals) are summarized in section III, which also presents qualitative comparisons with experiments³⁵ for mixtures of saturated polyisoprene or saturated poly(ethylbutadiene) with polypropylene. The computed miscibility patterns are also analyzed in terms of the entropic structural parameters (ESPs), which are trivial to compute and which enable predicting relative miscibilities for A_xB_{1-x}/A and A_xB_{1-x}/B systems with upper critical solution temperature phase diagrams. The latter feature is illustrated by comparing the ESPs for PEE_xPE_{1-x}/PP blends with observed miscibility trends^{16,36} as a function of copolymer composition x .

II. Model, Notation, and Basic Features of the Theory

The theory is designed to describe binary mixtures of a completely random copolymer A_xB_{1-x} and a homopolymer C . A single copolymer chain consists, on average, of n_A monomers of species A and n_B monomers of species B that are distributed randomly along the chain backbone. A chain with the average composition $x = n_A/(n_A + n_B)$ has these monomers joined by $(n_A + n_B - 1)$ backbone bonds. Each homopolymer chain is composed of n_C monomers of only one species which may be different or identical to one of the copolymer species A or B . The blend is represented as a set of n_1 and n_2 monodisperse chains of the random copolymer and homopolymer, respectively, by using an extended lattice model with a total of N_l lattice sites and a coordination number z .

The general theory is applicable to a wide class of systems, provided that individual A and B monomers of the random copolymer both have vinyl structures that spread over several lattice sites in order to represent the size, shape, etc., of the actual monomers. The treatment of other types of monomer structures by the LCT is possible but very tedious. Figure 1 depicts a few of the vinyl monomer structures that are considered in the computations. Applications to polyolefin systems assign individual CH_n ($n = 0, \dots, 3$) united atom groups to occupy single lattice sites.

The chain occupancy indices M_1 and M_2 are defined as $M_1 = n_A s_A + n_B s_B$ and $M_2 = n_C s_C$, where s_α designates the number of lattice sites occupied by a single monomer α . The values of s_A , s_B , and s_C are chosen to reflect the relative monomer sizes (see Table 1).

The existence of nonzero blend compressibility (i.e., of a nontrivial equation of state) implies the presence in the system of excess free volume, which is modeled by n_v empty sites with a volume fraction of $\phi_v \equiv n_v/N_l = 1 - (n_1 M_1 + n_2 M_2)/N_l = 1 - \phi_1 - \phi_2$. The excess free volume fraction ϕ_v is determined for a given pressure P , temperature T , and blend nominal composition $\Phi_1 = 1 - \Phi_2 = \phi_1/(1 - \phi_v)$ from the equation of state. The lattice is taken as a three-dimensional ($d = 3$) cubic lattice with $z = 2d = 6$.

Excluded volume constraints prohibit any two submonomer units from lying at the same lattice site and naturally represent the short range repulsive interactions. Longer range attractions are introduced by ascribing the attractive microscopic van der Waals energy $\epsilon_{\alpha\beta}^{ij}$ to the nearest neighbor (on the lattice) portions i and j of the monomers α and β . As described in subsection A, we employ the simplest interaction model in which all the s_α portions of a given monomer α are taken as energetically equivalent units. Thus,

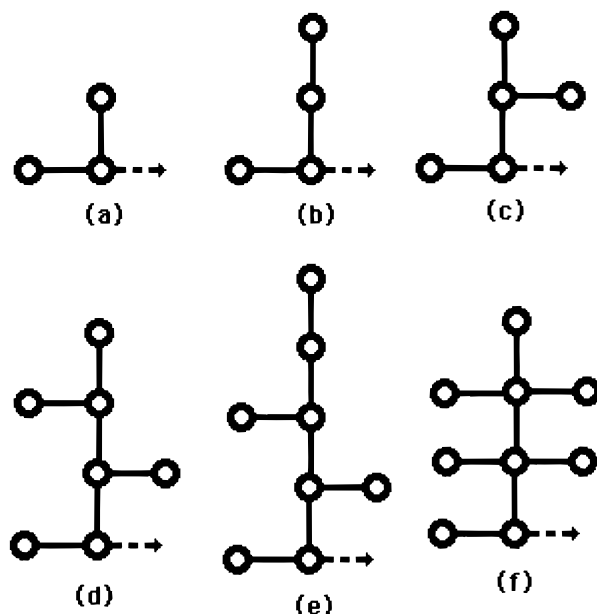


Figure 1. (a–e) United atom structures used as models for the monomer structures of several polyolefins. (b) Appropriate united atom structure for the vinyl methyl ether monomer. Monomers with the structure of diagram f appear in illustrative examples of LCT computations. Circles denote monomer portions that occupy single lattice sites, and arrows indicate the directions of linkages between consecutive monomers in the chains. The present random copolymer LCT cannot treat monomer structures with tetrafunctional backbone units.

Table 1. Monomer Site Occupancy Indices s_α and Numbers $s_\alpha^{(tri)}$ and $s_\alpha^{(tetr)}$ of Tri- and Tetrafunctional United Atom Groups, Respectively, in the Monomer Structures of Figure 1

monomer structure α	s_α	$s_\alpha^{(tri)}$	$s_\alpha^{(tetr)}$
a	3	1	0
b	4	1	0
c	5	2	0
d	7	3	0
e	8	3	0
f	9	1	2

these s_α subunits interact with any of the s_β portions of a monomer β with the same average energy $\epsilon_{\alpha\beta}$. Hence, the general model of an A_xB_{1-x}/C blend contains a minimum of six independent microscopic energetic parameters ϵ_{AA} , ϵ_{BB} , ϵ_{AB} , ϵ_{CC} , ϵ_{AC} , and ϵ_{BC} , producing a great complication over the treatment of compressible homopolymer binary blends. When $C = A$ or B , only three energetic parameters remain, as for binary A/B blends.

The generalized lattice model of random copolymer/homopolymer blends is solved²⁵ by using cluster expansion methods, which explicitly consider the short range correlations (and, hence, nonrandom mixing) that are present in polymer systems as a result of packing constraints and the different interactions $\{\epsilon_{\alpha\beta}\}$. The introduction of these local correlations into the theory enables²⁶ describing the sequence and monomer structure dependence of thermodynamic properties and, for instance, the different thermodynamic behaviors of random and alternating copolymer systems. The random copolymer version of a compressible generalization of FH theory emerges in the lattice cluster theory (LCT) as the zeroth order approximation.

The Helmholtz free energy F for the random copolymer blend is computed as a perturbative expansion

about the compressible FH free energy F^{FH} . The LCT free energy F is written²⁵ formally as

$$\frac{F}{N_1 k_B T} = \frac{F^{\text{FH}}}{N_1 k_B T} + \text{corrections} \quad (2.1)$$

where the corrections to the compressible system generalization of the FH approximation F^{FH} in eq 2.1 are derived as polynomials in the actual volume fractions ϕ_1 and ϕ_2 . The technical details and the diagrammatic representation of F are partially described elsewhere.^{25,26} The compressible system generalization of the FH free energy F^{FH} is given by

$$\frac{F^{\text{FH}}}{N_1 k_B T} = -\frac{S_{\text{com}}}{N_1 k_B T} - \frac{Z}{2} [\phi_1^2 (\epsilon_{\text{AA}} m_{\text{A}}^2 + \epsilon_{\text{BB}} m_{\text{B}}^2 + 2\epsilon_{\text{AB}} m_{\text{A}} m_{\text{B}}) + \phi_2^2 \epsilon_{\text{CC}} + 2\phi_1 \phi_2 (\epsilon_{\text{AC}} m_{\text{A}} + \epsilon_{\text{BC}} m_{\text{B}})] \quad (2.2)$$

where S_{com} denotes the combinatorial entropy, $m_{\alpha} = n_{\alpha} s_{\alpha} / (n_{\text{A}} s_{\text{A}} + n_{\text{B}} s_{\text{B}})$ designates the fraction of the random copolymer chain site occupancy index M_1 that is associated with monomers of species α , and the nearest neighbor van der Waals attractive energies $\{\epsilon_{\alpha\beta}\}$ are expressed in units of $k_B T$. The combinatorial entropy S_{com} contains an additional translational entropy term $\phi_v \ln \phi_v$ that accounts for the distribution of free volume in the system. When all three monomer occupancy indices are equal to unity, $s_{\text{A}} = s_{\text{B}} = s_{\text{C}} = 1$ (i.e., when the monomers are treated as structureless entities that occupy single lattice sites), and when the limit of infinite pressure ($\phi_v = 0$) is taken, eq 2.2 recovers the well-known random copolymer FH expression derived by Kambour *et al.*⁵ and ten Brinke *et al.*⁶,

$$\begin{aligned} \frac{F_{\text{inc}}^{\text{FH}}}{N_1 k_B T} &= \frac{\phi_1}{M_1} \ln \phi_1 + \frac{\phi_2}{M_2} \ln \phi_2 + \\ &\quad \phi_1 \phi_2 [x \chi_{\text{AC}} + (1-x) \chi_{\text{BC}} - x(1-x) \chi_{\text{AB}}] \quad (2.3) \\ &\equiv \frac{\phi_1}{M_1} \ln \phi_1 + \frac{\phi_2}{M_2} \ln \phi_2 + \phi_1 \phi_2 \chi_{\text{eff}} \end{aligned}$$

with $\chi_{\alpha\beta} = (Z/2)[\epsilon_{\alpha\alpha} + \epsilon_{\beta\beta} - 2\epsilon_{\alpha\beta}]$. The interesting physics summarized in eq 2.3 lies in the fact that the macroscopic interaction parameter χ_{AB} appears in the expression for χ_{eff} with a negative sign, thereby promoting blend miscibility for sufficiently "repulsive" A–B interactions.

Previous papers^{25,27} provide the details of the LCT for homopolymer blends as well as the necessary generalizations to random copolymer systems.²⁶ Thus, these lengthy details are omitted here.

A. Model for Polyolefin Blend Interaction Parameters. The simple FH type description of a compressible A/B binary polymer blend contains three macroscopic interaction parameters χ_{AA} , χ_{BB} , and χ_{AB} , which translate into three microscopic energy parameters ϵ_{AA} , ϵ_{BB} , and ϵ_{AB} in the minimal LCT model. The overall difficulty in assigning the three adjustable parameters is the same in both cases. Following the long-standing tradition in mixture theories, the LCT self-interaction energies ϵ_{AA} and ϵ_{BB} may be determined by applying the theory to reproduce thermodynamic data for melts of the individual pure components A and B, respectively, while the heterocontact energy ϵ_{AB} is subsequently fit to some experimental data for the A/B

mixture. The same three energy parameters are then available for describing the thermodynamic properties of A–b–B diblock copolymers and a variety of blends, such as A–b–B/A, A–b–B/A/B, $\text{A}_x\text{B}_{1-x}/\text{A}$, or $\text{A}_x\text{B}_{1-x}/\text{A}_y\text{B}_{1-y}$ mixtures. Sufficient experimental data for determining the interaction parameters are rarely accessible for the corresponding pure homopolymer binary polyolefin blends. An alternative approach would involve their extraction from, for example, equation of state data for random copolymer melts. Because the description of the random copolymer melt requires simultaneously fitting three monomer–monomer interaction energies (or two if the Berthelot approximation is invoked), extensive analysis and data for several samples with varying compositions are necessary in order to generate reliable values for ϵ_{AA} , ϵ_{BB} , and ϵ_{AB} . Data of this nature are most prevalent for hydrogenated poly(butadienes) (HPBs), but our LCT formulation currently cannot treat the monomer structures for the 1,4 HPB species. The situation, however, becomes more problematic for systems, such as $\text{A}_x\text{B}_{1-x}/\text{C}$ blends with $\text{C} \neq \text{A}$ or B , which are prominent among the experimentally studied^{15,16,35,36} polyolefin blends whose random copolymer character stems from the random addition of 1,2 and 1,4 units in the diene addition reactions. The theoretical treatment of these $\text{A}_x\text{B}_{1-x}/\text{C}$ blends requires introducing six interaction parameters, at a minimum, and these generally unavailable quantities are determined here from a very simple model, since our goal lies in probing general qualitative trends. Thus, in view of our primary goal of elucidating general microscopic molecular influences on copolymer miscibilities and of developing an "ultimate" interaction model, we introduce a zeroth order model for specifying all the interaction parameters for these systems. Those readers more interested in illustrative LCT computations and comparisons with experiment can skip to section III.

Our model is based on the use of Lennard-Jones well depths that have been determined in conjunction with extensive off-lattice simulations for alkanes and polyolefins. The simplest models employ Lennard-Jones potentials with different interaction parameters e_{ij} for homocontact interactions between pairs of CH, CH₂, CH₃, and C united atom groups, while more extensive treatments^{33,34} require that e_{ij} depend on, for example, whether a CH₃ group is bonded to a secondary, tertiary, and so forth carbon. All treatments,^{31–34} to our knowledge, choose the heterocontact interaction parameters e_{ij} as the Berthelot geometric mean despite the fact that the quantum mechanics of dispersion forces indicates this is but an approximation and that experiments for small molecule fluids exhibit its inadequacy.³⁷ While the geometric mean model is remarkably close to correct for many polyolefin blends,¹⁶ both simple analysis and LCT computations³⁸ indicate that very minor changes in e_{ij} from the geometric mean values of less than 1% can alter a binary blend from one that is predicted to be totally immiscible to one that is quite miscible. Given this strong reservation concerning the Berthelot combining rule, we adopt this approximation, along with the simplest models, in order to reduce the required number of interaction parameters to four ($e_{\text{CH}_3-\text{CH}_3}$, $e_{\text{CH}_2-\text{CH}_2}$, $e_{\text{CH}-\text{CH}}$, and $e_{\text{C}-\text{C}}$) which are sufficient to describe all polyolefin systems.

The problem is then how to convert a set of four off-lattice Lennard-Jones interaction parameters e_{ij} for the united atom groups of polyolefins into the four corre-

sponding lattice model interaction parameters ϵ_{ij} . We introduce a simple model based on the observation that most of the Lennard-Jones distance parameters σ_{ij} are generally quite similar^{31–34} for the different united atom groups. (The σ_{C-C} values sometimes differ significantly.³³) Thus, we first assume the equality of all the σ_{ij} values. Next, the nearest neighbor interaction energies are equated between the off-lattice and lattice models as follows: The lattice model interaction energy E_L is proportional³⁹ to

$$E_L \sim \sum_{i,j} \epsilon_{ij} g_{ij} \quad (2.4)$$

where g_{ij} is the nearest neighbor pair distribution function for i and j monomer portions that occupy single lattice sites. The subscripts i and j range over all united atom groups in the system. The corresponding total off-lattice energy⁴⁰ is

$$E_C \sim \sum_{i,j} \int_0^\infty d\mathbf{r} U_{ij}(\mathbf{r}|e_{ij}\sigma_{ij}) g_{ij}(\mathbf{r}) \quad (2.5)$$

where $U_{ij}(\mathbf{r}|e_{ij}\sigma_{ij})$ is the Lennard-Jones interaction, $g_{ij}(\mathbf{r})$ is the continuum pair distribution function, and all the $\sigma_{ij} \equiv \sigma$ are taken as equal. The interaction contains e_{ij} only as an overall factor $e_{ij}U(\mathbf{r}|\sigma)$, so this factor of e_{ij} may be removed from the integral. Approximating $g_{ij}(\mathbf{r})$ as the value for the nearest neighbor peak and assuming this $g_{ij}(\mathbf{r})$ to be identical to the lattice model g_{ij} , the nearest neighbor portion of E_C is equivalent to the lattice model approximation E_L if ϵ_{ij} is equated to the integral of $U(\mathbf{r}|\sigma_{ij})$ over a first neighbor shell. Because the same σ_{ij} appears for all interactions, the latter integral is e_{ij} times a universal constant. Thus, these admittedly very crude arguments suggest a zeroth order model in which ϵ_{ij} and e_{ij} are proportional to each other,

$$\epsilon_{ij} = C e_{ij} \quad (2.6)$$

with C the single adjustable constant.

A recent work⁴¹ provides a general formulation of the LCT in which each united atom group within a monomer is permitted to interact with a different energy. However, this LCT formulation is currently lacking for the more complex random copolymer systems. Moreover, since the available data for polyolefin blends contain too few examples with both components being pure homopolymers that are free of random microstructure, we are forced to invoke the further approximation of averaging the interaction parameters over all sites occupied by individual monomers. These monomer-averaged interaction parameters are obtained as

$$e_{\alpha\alpha} = \frac{1}{s_\alpha} \sum_{k,l=1}^{s_\alpha} e_{kl} \quad (2.7)$$

and

$$e_{\alpha\beta} = \frac{1}{s_\alpha s_\beta} \sum_{k=1}^{s_\alpha} \sum_{l=1}^{s_\beta} e_{kl} \quad (2.8)$$

where s_α and s_β denote the site occupancy indices for monomers of species α and β , respectively. The subscripts k and l range over all united atom groups within an individual monomer. The simple scaling of eq 2.6 is

also invoked between the monomer-averaged energy parameters $\epsilon_{\alpha\beta}$ and $e_{\alpha\beta}$,

$$\epsilon_{\alpha\beta} = C e_{\alpha\beta} \quad (2.9)$$

Equations 2.7–2.9 enable determining all three $\epsilon_{\alpha\beta}$ values for $A_x B_{1-x}/A(B)$ mixtures and all six $\epsilon_{\alpha\beta}$ values for $A_x B_{1-x}/C$ systems, based only on the off-lattice Lennard-Jones parameters e_{ij} and the constant C of eq 2.9, which is determined from an earlier fit⁴² of the LCT to PVT data for PP and hhPP melts ($\epsilon_{P-P} = 202.19$ K and $\epsilon_{hP-hP} = 208.60$ K). For example, choosing the set of Lennard-Jones parameters given by Mondello *et al.*³¹ ($e_{CH_3-CH_3} = 114$ K, $e_{CH_2-CH_2} = 47$ K, and $e_{CH-CH} = 40$ K), we obtain $C = 3.39$.

Considering the nature of the approximations involved, the interaction parameters are suitable only for qualitative analysis. Three other sets of Lennard-Jones parameters^{32–34} have also been used, and all three sets yield qualitatively similar patterns of miscibility. Likewise, we have examined models with weight factors inserted into summands in eqs 2.7 and 2.8 in order to account for the differing functionalities (i.e., “surface fractions”) of the united atom groups, again with no qualitative changes. A major effort will be involved in relaxing the crude assumptions of the interaction model and in the semiempirical determination of an optimal set of LCT polyolefin interaction parameters $\epsilon_{\alpha\beta}$ which we expect would exhibit small but qualitatively significant deviations from the geometric combining rule. Comparisons with experiment based on the simple model in eqs 2.7–2.9 are useful in guiding the future determination of optimal interaction energies.

III. Computations of Constant Pressure Spinodals

Constant pressure spinodal curves, which determine the homogeneous one-phase stability limits, are calculated for random copolymer/homopolymer blends by employing the LCT Helmholtz free energy F from eq 2.1. The general procedure is explained in our earlier papers.^{20,43} The constant pressure condition more accurately describes the majority of experiments. Binodals have also been computed and are presented in Figure 2 for illustration, since our interest lies in probing general trends which are elucidated by *either* binodals or the slightly easier to compute spinodals. The excess free volume fraction ϕ_v is determined from the equation of state, and the unit cell volume v_{cell} associated with a single lattice site is assumed to be a constant ($v_{cell} = 2.5477^3$ Å³). The energetic parameters $\{\epsilon_{\alpha\beta}\}$ are assigned to illustrate general trends or are estimated using the model described in section II.

Subsection A describes the computed phase diagrams for examples of symmetric $A_x B_{1-x}/A$ and $A_x B_{1-x}/B$ blends with $x = 0.5$ and with upper or lower critical solution temperatures (LCSTs) and even with both. Because disparities in miscibilities between $A_{0.5}B_{0.5}/A$ and $A_{0.5}B_{0.5}/B$ systems depart from the predictions of random copolymer FH theory (see eq 2.3), the computed differences are then analyzed in terms of the structural asymmetry of the blend components. Subsection C summarizes computations for $A_x B_{1-x}/C$ binary mixtures where the three binary homopolymer blends A/B , A/C , and B/C are completely immiscible, but the random copolymer $A_x B_{1-x}$ mixes with homopolymer C reasonably well over wide ranges of compositions x and Φ_1 .

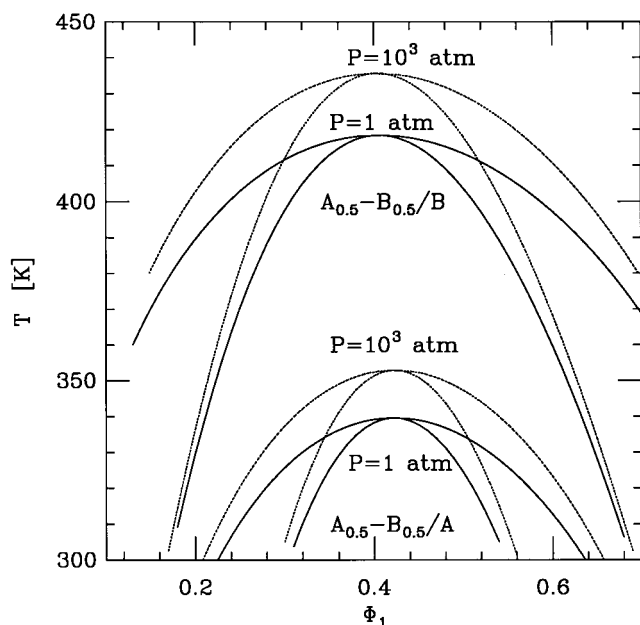


Figure 2. Computed LCT spinodal and binodal curves for model UCST $A_{0.5}B_{0.5}/A$ and $A_{0.5}B_{0.5}/B$ mixtures at $P = 1$ and 1000 atm. The polymerization indices of the two polymer blend species are $N_1 \equiv n_A + n_B = 120$ and $N_2 = 120$ for the $A_{0.5}B_{0.5}/A$ blend and $N_1 = N_2 = 80$ for the $A_{0.5}B_{0.5}/B$ system. The subscript 1 labels the random copolymer, while the subscript 2 refers to the homopolymer. The same convention is employed in Figures 3, 4, and 6–8.

While this type of behavior is predicted by a modification of incompressible random copolymer FH theory to include the temperature independent portion of χ , a much richer array of phase diagrams, as well as the important pressure dependence, is predicted from our random copolymer LCT computations. Subsection D presents comparisons with experiments^{16,35,36} for polyolefin systems.

A. Spinodals for $A_{0.5}B_{0.5}/A$ and $A_{0.5}B_{0.5}/B$ Blends.

We begin analyzing the miscibility of $A_{0.5}B_{0.5}/A$ and $A_{0.5}B_{0.5}/B$ blends by considering mixtures exhibiting UCST phase diagrams. The present calculations employ the microscopic van der Waals energies³⁸ $\epsilon_{A-A} = 0.62k_B T_0$, $\epsilon_{B-B} = 0.593k_B T_0$, and $\epsilon_{A-B} = 0.6051208k_B T_0$ ($T_0 = 415.15$ K) as representative of many other choices of $\{\epsilon_{ij}\}$ that produce a positive exchange energy. The monomers A and B are depicted, respectively, by structures f and d of Figure 1. The computed spinodals in Figure 2 indicate that the LCT predicts very different miscibilities for these two systems, in contrast to FH type approximations which do not distinguish between $A_{0.5}B_{0.5}/A$ and $A_{0.5}B_{0.5}/B$ mixtures. Figure 2 also demonstrates the influence of pressure on the miscibility of UCST A_xB_{1-x}/A and A_xB_{1-x}/B systems. An increase in pressure renders both systems less miscible, a trend quite typical in LCT computations for UCST binary homopolymer blends.²⁰ A more significant pressure dependence of miscibility appears in Figures 3 and 4. Binodal curves are also included in Figure 2, but they provide no new general insights into miscibility patterns beyond those evident from the spinodals. Thus, to avoid clutter in subsequent figures, we present only the spinodals.

Figure 3 illustrates the generic behavior of LCST $A'_{0.5}B'_{0.5}/A'(B')$ random copolymer systems. The structures f and b of Figure 1 are taken to represent, respectively, the A' and B' monomers. The spinodals

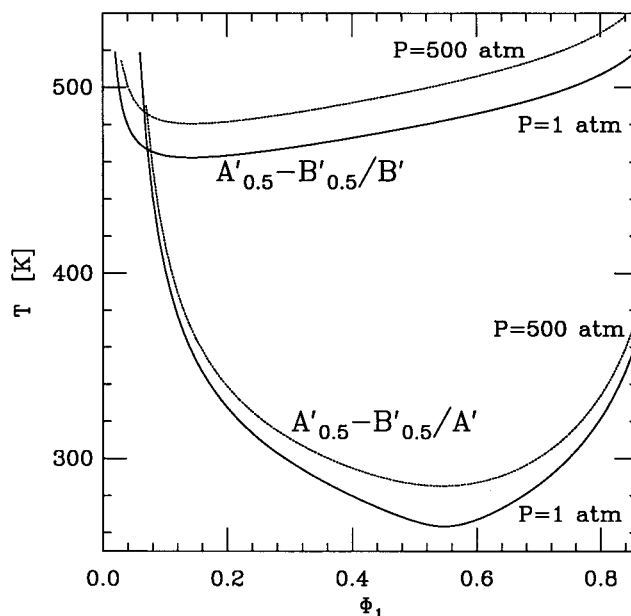


Figure 3. Computed LCT spinodal curves for model LCST $A'_{0.5}B'_{0.5}/A'$ and $A'_{0.5}B'_{0.5}/B'$ mixtures at $P = 1$ and 500 atm. The polymerization indices for the two polymer blend species are $N_1 \equiv n_A + n_B = 6000$ and $N_2 = 3000$.

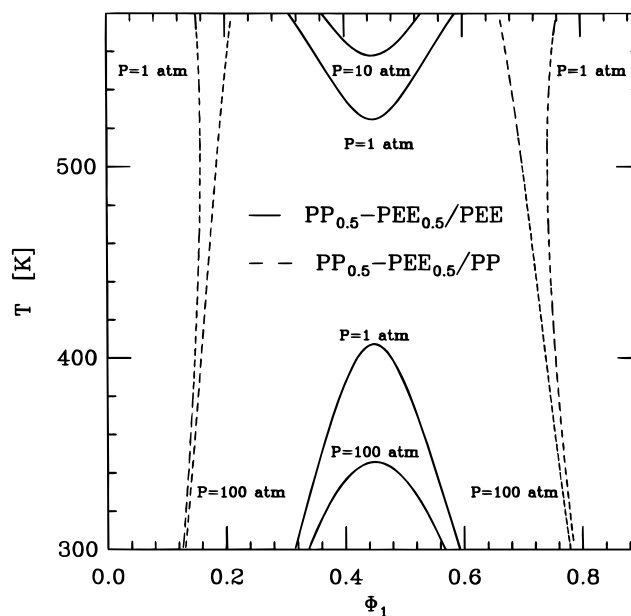


Figure 4. Computed LCT phase boundaries for $PP_{0.5}PEE_{0.5}/PP$ and $PP_{0.5}PEE_{0.5}/PEE$ mixtures at $P = 1$ and 100 atm (and only 10 atm for the top curve). The polymerization indices for the two polymer blend species are $N_1 \equiv n_A + n_B = 2000$ and $N_2 = 1200$. The monomer average van der Waals attractive interaction energies ($\epsilon_{P-P} = 0.5164k_B T_0$, $\epsilon_{EE-EE} = 0.4814k_B T_0$, and $\epsilon_{P-EE} = 0.4986k_B T_0$, $T_0 = 415.15$ K) are determined from the interaction model of section II.A and also apply to Figures 5 and 6.

in Figure 3 are computed by employing a prior set³⁸ of three van der Waals energies [$\epsilon_{A'-A'} = 0.62k_B T_0$, $\epsilon_{B'-B'} = 0.59k_B T_0$, and $\epsilon_{A'-B'} = 0.607675k_B T_0$ ($T_0 = 415.15$ K)], but other choices of energy parameters that yield a negative exchange energy do not alter the general trends in Figure 3. Again, Figure 3 displays different miscibilities of the symmetric random copolymer with a homopolymer of either copolymer species. An increased pressure leads to the opposite behavior than that presented in Figure 2 for a UCST system. Elevat-

ing the pressure is predicted to enhance the blend miscibility for the LCST random copolymer/homopolymer systems in Figure 3, as it does in LCT calculations for typical LCST homopolymer blends.³⁸

LCT computations for other $A_xB_{1-x}/A(B)$ systems display both lower and upper critical solution temperature phase diagrams. This behavior is illustrated in Figure 4, which depicts spinodals for $PP_{0.5}PEE_{0.5}/PP$ and $PP_{0.5}PEE_{0.5}/PEE$ mixtures, where the random copolymer could be made with metallocene catalysts from mixtures of propylene and butene-1. The propylene and ethyl-ethylene monomers are represented, respectively, by the united atom structures a and b of Figure 1, and the three microscopic van der Waals energies $\epsilon_{P-P} = 0.5164k_B T_0$, $\epsilon_{EE-EE} = 0.4814k_B T_0$, and $\epsilon_{P-EE} = 0.4986k_B T_0$, are obtained by using the interaction model described in section II.A and the Lennard-Jones parameters given by Mondello *et al.*³¹

An analysis of the spinodals in Figure 4 leads to several important observations. Firstly, the computed miscibility of the symmetric random copolymer $PP_{0.5}PEE_{0.5}$ with PEE strongly exceeds its miscibility with PP. Secondly, blending the symmetric random copolymer $PP_{0.5}PEE_{0.5}$ with PEE or with PP yields two qualitatively different miscibility patterns. One pattern (for $PP_{0.5}PEE_{0.5}/PEE$) involves both upper and lower critical solution temperatures, while another (for $PP_{0.5}PEE_{0.5}/PP$) contains an hourglass miscibility gap without a critical temperature. As exhibited in Figures 5 and 6, similar phase behaviors also appear in LCT computations for PP/PEE homopolymer blends with different molecular weights and for PP_xPEE_{1-x}/PEE random copolymer/homopolymer mixtures with different random copolymer compositions x , respectively. Thirdly, small applied pressures of only 10 or 100 atm improve the compatibility of PP_xPEE_{1-x}/PP and PP_xPEE_{1-x}/PEE blends by shrinking the miscibility gap or by displacing the LCST and UCST branches of the phase diagram from each other (see Figure 4). Similar pressure dependent shifts in miscibility are predicted by LCT computations for PP/PEE homopolymer blends.

The PP_xPEE_{1-x}/PP case illustrates trends present in numerous other LCT computations. This example is also useful because the predictions of limited miscibility for PE/PEE mixtures (see Figure 5) disagree completely with experiments.¹⁶ The fact that PP/H97 blends are found¹⁶ to be miscible in the range of molecular weights used in Figure 5 indicates a deficiency of our simple model for the interaction energies and motivates more a detailed fitting of these energies to experimental data, as discussed above.

B. Entropic Factors. The examples of Figures 2–4 clearly demonstrate the LCT prediction of generally significantly different miscibilities for the symmetric random copolymer A_xB_{1-x} with homopolymers of species A or B. Since the same three interaction energy parameters ϵ_{AA} , ϵ_{BB} , and ϵ_{AB} are common to the LCT description of both $A_{0.5}B_{0.5}/A$ and $A_{0.5}B_{0.5}/B$ blends, the computed disparities in the miscibilities of these two systems emerge, in part, from entropic factors, as now explained. The entropic portion $\chi_{\text{eff}}^{(S)}$ of the effective interaction parameter χ_{eff} is one standard measure of the “entropic effects” in a polymer system. This $\chi_{\text{eff}}^{(S)}$ arises in the LCT from constraints on packing monomers with differing sizes and shapes. The LCT $\chi_{\text{eff}}^{(S)}$ exhibits²⁷ a simple analytical form in the athermal limit of infinite molecular weights ($M_1, M_2 \rightarrow \infty$) and pres-

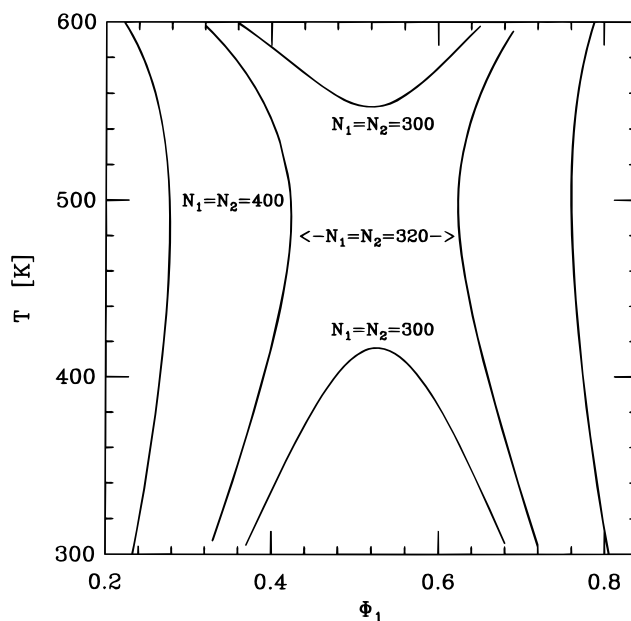


Figure 5. Computed LCT phase boundaries for PP/PEE homopolymer blends (at $P = 1$ atm) with different molecular weights, as indicated in the figure. The subscript 1 labels PP.

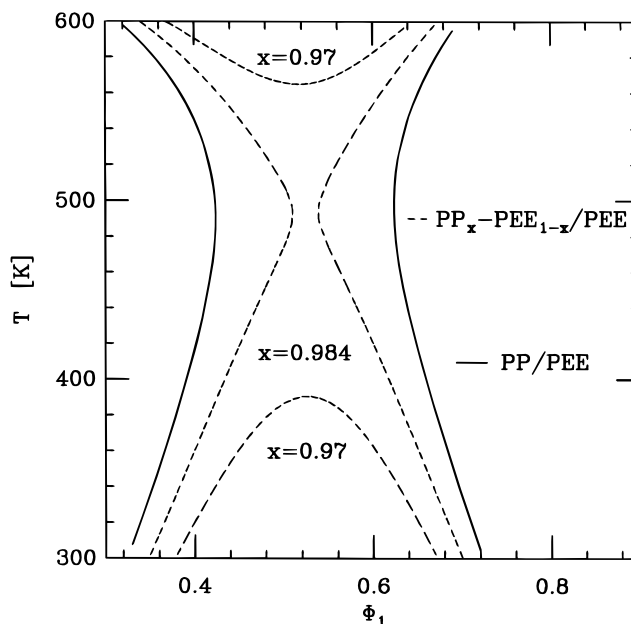


Figure 6. Computed LCT phase boundaries for PP_xPEE_{1-x}/PEE blends (at $P = 1$ atm) with the same polymerization indices $N_1 = N_2 = 320$ but different compositions x of the random copolymer. The spinodal for the limiting case of $x = 1$, that is, for the PP/PEE system, is also presented for comparison.

sures ($P \rightarrow \infty$),

$$\chi_{\text{eff}}^{(S)} = \frac{1}{z^2} \left[\frac{N_2^{(1)}}{M_1} - \frac{N_2^{(2)}}{M_2} \right]^2 \quad (3.1)$$

where the geometrical coefficient $N_2^{(i)}$ designates the number of ways for selecting two sequential bonds in a single chain of polymer species i ($i = 1, 2$) and z denotes the lattice coordination number. (A simpler representation of the $N_2^{(i)}$ is used below.) The formula 3.1 applies to arbitrary binary blends with any combination of homopolymers, diblock copolymers, random copolymers, and so forth.

The entropic structural parameter (ESP),

$$r \equiv |r_1 - r_2| = |N_2^{(1)}/M_1 - N_2^{(2)}/M_2| \quad (3.2)$$

which appears squared in eq 3.1, has been suggested by us to be a general measure of blend structural asymmetry. For example, the ESP has been used as a successful predictor of blend miscibility in LCT computations^{20,21} for model upper critical solution temperature polyolefin blends where identical interactions are taken to apply between all united atom groups of both species. A smaller r implies a smaller $\chi_{\text{eff}}^{(S)}$ and, hence, better miscibility.

The ratios $r_1 \equiv N_2^{(1)}/M_1$ for the A_xB_{1-x} random copolymer, labeled as species 1, and $r_2 \equiv N_2^{(2)}/M_2$ for the homopolymer C, denoted as species 2, may be expressed more conveniently as

$$\frac{N_2^{(1)}}{M_1} = \frac{[s_A + s_A^{(\text{tri})} + 3s_A^{(\text{tet})}]x + [s_B + s_B^{(\text{tri})} + 3s_B^{(\text{tet})}](1-x)}{s_A x + s_B(1-x)} \quad (3.3a)$$

and

$$\frac{N_2^{(2)}}{M_2} = \frac{s_C + s_C^{(\text{tri})} + 3s_C^{(\text{tet})}}{s_C} \quad (3.3b)$$

where s_A , s_B , and s_C are the numbers of sites occupied by monomers of the respective species, and Table 1 summarizes the $s_A^{(\text{tri})}$ and $s_A^{(\text{tet})}$ for all the monomers depicted in Figure 1. Equation 3.3b follows from eq 3.3a by taking the limit $x = 1$ and by substituting the subscript C for the subscript A.

The relations in eqs 3.3a and 3.3b enable evaluating the blend entropic structural parameters r for all six model blends whose phase diagrams are depicted in Figures 2–4, as well as for other systems of random copolymers with tetrafunctional backbone units. The calculation just involves the trivial counting of different types of united atom units in the monomer structures of both blend species. The results for the systems of Figures 2–4 are written in the form of inequalities

$$r(A_{0.5}B_{0.5}/A) = 0.1528 < r(A_{0.5}B_{0.5}/B) = 0.1964$$

$$r(A'_{0.5}B'_{0.5}/A') = 0.1624 < r(A'_{0.5}B'_{0.5}/B') = 0.3654$$

and

$$r(\text{PP}_{0.5}\text{PEE}_{0.5}/\text{PEE}) = 0.0357 < r(\text{PP}_{0.5}\text{PEE}_{0.5}/\text{PP}) = 0.0476$$

in order to indicate the expected trends in the blend miscibilities. The miscibility patterns presented in Figures 2 and 4 exactly confirm the trends derived on the basis of the magnitude of $\chi_{\text{eff}}^{(S)}$ or r . The spinodals in Figure 3 demonstrate that a lower r does not necessarily imply a better miscibility for LCST $A'_{0.5}B'_{0.5}/A'(B')$ systems, but the correlation of blend miscibility with r has only been derived^{20,21} for UCST systems for which energetic parameters are very similar.

C. Spinodals for A_xB_{1-x}/C Systems. Explaining the miscibilities of an A_xB_{1-x} random copolymer with a

distinct homopolymer $C \neq A$ or B has been a long-standing theoretical challenge. The simple FH random copolymer theory^{5,6} of eq 2.3 predicts that the A_xB_{1-x}/C systems ($C \neq A, B$) are completely miscible over the range $x_1 \leq x \leq x_2$ with

$$x_1 \equiv \frac{-(\chi_{AC} - \chi_{BC} - \chi_{AB}) - [(\chi_{AC} - \chi_{BC} - \chi_{AB})^2 - 4\chi_{AB}\chi_{BC}]^{1/2}}{2\chi_{AB}} \quad (3.4a)$$

and

$$x_2 \equiv \frac{-(\chi_{AC} - \chi_{BC} - \chi_{AB}) + [(\chi_{AC} - \chi_{BC} - \chi_{AB})^2 - 4\chi_{AB}\chi_{BC}]^{1/2}}{2\chi_{AB}} \quad (3.4b)$$

for which the effective interaction parameter χ_{eff} of eq 2.3 is negative. Incompatibility between homopolymers of species A and B facilitates the miscibility of an A_xB_{1-x} random copolymer with a homopolymer C, even when the A/C and B/C binary blends themselves are incompatible. This fascinating and technologically important feature of random copolymer blend thermodynamics is also present in the LCT, which, however, yields a much richer array of miscibility patterns than those emerging from simple FH type theories.

This subsection summarizes LCT computations of the phase diagrams for a family of A_xB_{1-x}/C polyolefin mixtures having vinyl monomer structures for all three species A, B, and C and displaying a vanishing FH effective interaction parameter χ_{eff} (for some x) as calculated using the simple interaction model of section II.A. Examples with negative χ_{FH} would be even more illustrative, but the present model does not predict negative χ_{FH} for any of the four literature sets of L-J well depths, probably as a consequence of using the Berthelot combining rule and, perhaps, of monomer-averaged interaction energies.

Figures 7 and 8 display the computed LCT spinodal curves generated for A_xB_{1-x}/C polyolefin mixtures whose A, B, and C monomers are represented, respectively, by structures a, c, and e of Figure 1. The van der Waals attractive energies are obtained from the polyolefin interaction model of section II.A as $\epsilon_{AA} = 0.51640959k_B T_0$, $\epsilon_{BB} = 0.54529115k_B T_0$, $\epsilon_{AB} = 0.53065392k_B T_0$, $\epsilon_{CC} = 0.53436848k_B T_0$, $\epsilon_{AC} = 0.52531230k_B T_0$, and $\epsilon_{BC} = 0.53980219k_B T_0$ ($T_0 = 415.15$ K). The large number of significant digits for these $\epsilon_{\alpha\beta}$ values is necessary to ensure that the FH χ_{eff} of eq 2.3 vanishes (for some x), and the above example is typical of many that produce a nearly vanishing χ_{eff} . The compositions x_1 and x_2 of eqs 3.4a and 3.4b are determined as $x_1 = x_2 = 0.375$.

The LCT spinodals in both Figures 7 and 8 exhibit a rich variety of phase behaviors. The phase diagram changes from an hourglass miscibility gap without a critical temperature (for $x \leq 0.35$) to a two-branch form with both upper and lower critical temperatures. A further increase in x (i.e., in the percentage of species A in the A_xB_{1-x} random copolymer), leads to the presence of only a lower critical solution temperature which gradually disappears with increasing x , reflecting complete miscibility. A small closed loop appears in Figure 8 when $x = 0.58$, providing a first signal of degrading blend miscibility with further increasing x . Two other patterns in Figure 8 correspond to $x = 0.6$ and $x = 0.64$ and exhibit only one critical solution temperature. Both

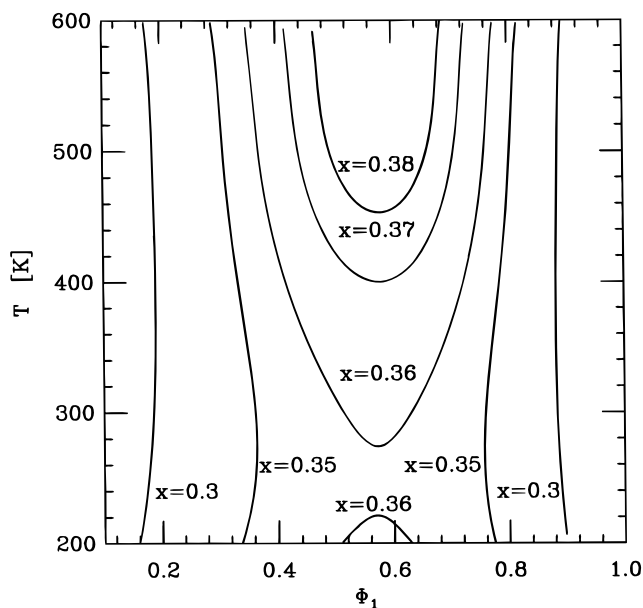


Figure 7. Computed LCT phase boundaries for A_xB_{1-x}/C polyolefin blends (at $P = 1$ atm) with the same polymerization indices $N_1 = N_2 = 17\,500$ but different compositions x of the random copolymer. The monomers for the A, B, and C species are represented, respectively, by the united atom structures a, c, and e of Figure 1. The energy parameters $\{\epsilon_{\alpha\beta}\}$ (determined from the interaction model of section II.A) are cited in the text.

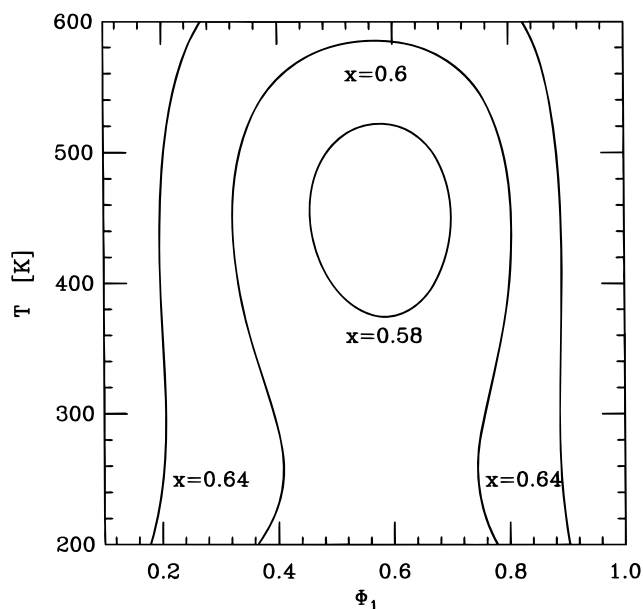


Figure 8. Same as Figure 7 for different ranges of composition x .

these patterns indicate a further diminution of miscibility. The rich behavior illustrated in Figures 7 and 8 is quite typical of LCT computations for A_xB_{1-x}/C polyolefin blends with a vanishing FH χ_{eff} that are constructed from the more extended list of monomer structures in Figure 1 of ref 27.

D. Qualitative Comparisons with Experiment.

Recent experiments of Reichart *et al.*³⁵ for binary blends of polypropylene (PP) with either saturated poly(ethylbutadiene) (sPEB) or saturated polyisoprene (sPI) reveal negative SANS interaction parameters χ and negative slopes α in plots of $\chi(1/T)$ versus $1/T$. On this basis, the authors suggest³⁵ that these systems exhibit LCST

behaviors with critical temperatures in excess of 300 °C. Invoking the standard stability condition (for an incompressible model)

$$\frac{1}{N_1\Phi_1} + \frac{1}{N_2\Phi_2} - 2\left(\chi^{(S)} + \frac{\alpha}{T}\right) = 0$$

where the entropic component $\chi^{(S)}$ is obtained by extrapolating the SANS χ to $1/T = 0$, enables us to estimate the spinodal temperatures as $T_s(\Phi_1 = 0.5) = 750$ and 784 K for the two experimental sPEB/PP blend samples. These high temperatures and the lack of a positive extrapolated T_s for the sPI/PP system conform to the previous observation that these mixtures are highly miscible. Similar miscibility patterns are found in a number of LCT computations and are illustrated in Figures 7 and 8 for model A_xB_{1-x}/C blends.

The saturated poly(ethylbutadiene) and polyisoprene samples used in the SANS experiments³⁵ are both random copolymers from the random addition of 3,4 and 1,4 units followed by saturation with hydrogen or deuterium. The samples contain 50% of each isomeric species. The high percentages of the two isomers also imply that the sPEB/PP and sPI/PP blends should be treated as A_xB_{1-x}/C random copolymer/homopolymer systems, rather than as D/C homopolymer blends, in order to extract meaningful thermodynamic and microscopic information from the measurements. The LCT computations suggest that the negative χ parameter observed in the SANS experiments and the related very high miscibility both can readily stem from the domination of "repulsive" A–B interactions over those between AC and BC monomer pairs, a situation quite often occurring in A_xB_{1-x}/C random copolymer mixtures. On the other hand, a simple calculation of the FH effective interaction parameter χ_{eff} from the interaction model of section II.A (with three different sets^{31–34} of Lennard-Jones parameters) does not produce a negative χ_{eff} for either system. There are several possible sources of this deficiency. Bearing in mind that the SANS χ and the FH χ_{eff} are, generally, not the same quantities, we note that both blends in the SANS experiments³⁵ are partially deuterated, and the model of section II.A, as a first approximation, does not account for this effect on the SANS intensities or for other potential complexities (e.g., not purely random microstructure) in the experimental samples. The use of the Berthelot geometric mean rule and, perhaps, of monomer-averaged interaction energies appears to be the main source of the above limitation of the interaction model. Moreover, additional LCT computations (not shown) for several other model A_xB_{1-x}/C polyolefin blends indicate that a negative or nearly vanishing FH χ_{eff} is not even necessary to generate a LCST phase diagram or a full miscibility region. Unfortunately, the limitation of the present theory to systems with vinyl monomers containing side groups and no tetrafunctional backbone units precludes applications of the LCT to compute spinodals for the united atom structure mixtures appropriate to sPEB/PP and sPI/PP blends. Thus, we can only consider qualitative comparisons with the experimental data of Reichart *et al.*³⁵

The entropic structural parameters (ESPs) provide a qualitative measure of how miscibilities of A_xB_{1-x}/C blends vary with the composition of A_xB_{1-x} random copolymers, as we now illustrate by comparing them with experimental data^{16,36} for mixtures of polypropyl-

ene (PP) with hydrogenated (or deuterated) polybutadienes (designated $\text{PEE}_x\text{PE}_{1-x}$ following the notation used in ref 36). The former are typical random copolymers due to random addition of 1,2 and 1,4 units. Applying eq 3.3b to a PP monomer with $s_{\text{PP}} = 3$ united atom groups in each PP monomer yields $r_1 \equiv r_{\text{PP}} = 4/3$, since $s_{\text{PP}}^{(\text{tri})} = 1$ and $s_{\text{PP}}^{(\text{tet})} = 0$ (see Table 1). The hydrogenated butadiene units from 1,2 or 1,4 additions have the same numbers of united atom groups ($s_{\text{PE}} = s_{\text{PEE}} = 4$) but vary in the numbers of trifunctional carbons ($s_{\text{PE}}^{(\text{tri})} = 0$ versus $s_{\text{PEE}}^{(\text{tri})} = 1$). Thus, eq 3.3a produces $r_2 = 1 + x/4$. The entropic structural parameter $r = |r_1 - r_2| = |1/3 - x/4|$ ranges from a maximum of $r(x=0) = 1/3$ for PP/PE blends to $r(x=1) = 1/6$ for PP/PEE mixtures, indicating an increased miscibility of $\text{PEE}_x\text{PE}_{1-x}$ /PP systems as x grows, in conformity with the experimental observations of Graessley *et al.*¹⁶ and Weimann *et al.*³⁶

IV. Discussion

Section I already emphasized the importance of devising a theory that accounts for the differences in thermodynamic properties induced by monomer molecular structures, as well as differences for various types of copolymers, such as random, alternating, diblock, etc., copolymer systems, with the same monomer compositions x . These respective differences arise naturally in the LCT from the use^{25,27} of the extended lattice model and from the monomer sequence dependent contributions to the LCT free energy which, in turn, appear²⁶ because the theory describes the local correlations (i.e., nonrandom mixing) induced by packing constraints and by different monomer–monomer interactions.

The numerical applications of the LCT in section III treat two broad classes of random copolymer/homopolymer blends. The first group contains mixtures of the symmetric random copolymer A_xB_{1-x} ($x = 0.5$) with a homopolymer of either species A or B, whereas the second group involves homopolymers of a species $C \neq A$ or B. While standard random copolymer FH theory predicts identical phase diagrams for the $\text{A}_{0.5}\text{B}_{0.5}/\text{A}$ and $\text{A}_{0.5}\text{B}_{0.5}/\text{B}$ systems, the LCT indicates that both systems may exhibit significantly differing miscibilities. Indeed, we choose as a particular illustration an example that displays wholly different phase behaviors for these two systems. The disparities in the computed miscibilities are partially explained in terms of the structural asymmetry of the blend components, an asymmetry that is characterized by differences in the LCT entropic structural parameter r .

We are unable to describe $\text{PS}_x\text{PMMA}_{1-x}/\text{PS}$ and $\text{PS}_x\text{PMMA}_{1-x}/\text{PMMA}$ blends in order to make comparisons with experiments^{8,30} for these systems because the current theory cannot provide the leading monomer sequence dependent contributions to the free energy when both random copolymer monomers are large and bulky. Thus, further theoretical studies are necessary to treat these systems.

$\text{A}_x\text{B}_{1-x}/\text{C}$ blends are described by the LCT as systems exhibiting a rich variety of miscibility patterns, depending on the composition x of the random copolymer, the monomer structures, and the interaction energies. Figures 7 and 8 exhibit the enormous variability of the phase diagram with composition x for but a single system. The behavior in these figures is not unique and is chosen for a case in which the three binary homopoly-

mer blends A/B, A/C, and B/C are completely immiscible but the random copolymer A_xB_{1-x} mixes reasonably well for some range of x with homopolymer C due to a vanishing effective FH interaction parameter $\chi_{\text{FH}} \equiv x\chi_{\text{AC}} + (1-x)\chi_{\text{BC}} - x(1-x)\chi_{\text{AB}}$ for $x = 0.375$ and due to a vanishing entropic structural parameter r for $x = 0.5$. This rich variation of the phase diagram with x is clearly outside the predictive possibilities of the random copolymer FH theory. As the composition x varies, the LCT computations yield phase boundaries with upper or lower critical solution temperatures, with both of them, and finally even without a critical point.

The realization that many polyolefin blends are random copolymer systems sheds light on simple interpretations for previously puzzling thermodynamic data.³⁵ For instance, consider the high miscibilities of sPEB/PP and sPI/PP blends as estimated³⁵ from the observation of negative SANS effective interaction parameters χ_{eff} . These systems need not be regarded as anomalous³⁵ when it is recognized that they are both $\text{A}_x\text{B}_{1-x}/\text{C}$ random copolymer mixtures. The observed behavior may indeed arise when the A–B “repulsive” interactions are dominant (see eq 2.3). A better interaction model than that sketched in section II.A is, however, necessary for a more quantitative analysis.

Because of the analytical complexity of the full LCT, we also consider a simple approach generated by appending the LCT athermal entropic limit $\chi_{\text{eff}}^{(\text{S})}$ of eq 3.1 to the random copolymer FH interaction parameter χ_{FH} . Our previous paper⁷ introduces an *ad hoc* model of $\chi_{\text{eff}}^{(\text{S})}$ for random copolymer systems based on interpolation between known homopolymer limits. A byproduct of the present work is an explicit but very simple expression (devoid of adjustable parameters) for the $\chi_{\text{eff}}^{(\text{S})}$ appropriate to random copolymer blends. This $\chi_{\text{eff}}^{(\text{S})}$ may be used as a simple tool for interpreting thermodynamic data for certain random copolymer blends. The introduction of $\chi_{\text{eff}}^{(\text{S})}$ does not eliminate the insensitivity of FH theory to the monomer sequence, but it enables describing blends with LCST phase diagrams, while still maintaining the simplicity and the interesting physics involved in the random copolymer FH mean field approximation. The phase behaviors displayed by the full LCT are only partially mirrored by this simpler model (compressible FH theory with $\chi_{\text{eff}}^{(\text{S})}$) because this simpler theoretical approach cannot reproduce the LCT computations for phase diagrams with both upper and lower critical temperatures. This limitation arises because of the absence of LCT contributions of order ϵ^2 in the FH free energy.

We employ a simple model for the interaction energies based on off-lattice Lennard-Jones interactions taken from united atom model simulations of alkane systems (including polymers). While the use of this interaction model suffices to exhibit general trends expected for polyolefins (based on many more examples than presented), comparisons with experiments for PP/PEE homopolymer blends demonstrate the inadequacy of this approach for any of the sets of Lennard-Jones used. Thus, further comparisons with experiment must confront the problem of fitting several interaction energies to experimental data.

Acknowledgment. We are grateful to Jack F. Douglas for critical reading of the manuscript and to Ilja Siepmann for sending values of Lennard-Jones

interaction parameters prior to publication. This research is supported, in part, by NSF Grant No. DMR-9530403.

References and Notes

- (1) Traugott, T. D. In *Concise Encyclopedia of Polymer Science and Engineering*; Kroschwitz, J. I., Ed.; Wiley: New York, 1990; p 1119.
- (2) Paul, D. R.; Barlow, J. W. *Polymer* **1984**, *25*, 487.
- (3) Roe, R. J.; Rigby, D. *Adv. Polym. Sci.* **1987**, *82*, 103. Huh, W.; Karasz, F. E. *Macromolecules* **1992**, *25*, 1057.
- (4) Sakurai, S.; Hasegawa, H.; Hashimoto, T.; Hargis, I. G.; Aggarwal, S. L.; Han, C. C. *Macromolecules* **1990**, *23*, 451. Sakurai, S.; Izumitani, T.; Hasegawa, H.; Hashimoto, T.; Han, C. C. *Macromolecules* **1991**, *24*, 4844. Sakurai, S.; Jinnai, H.; Hasegawa, H.; Hashimoto, T.; Han, C. C. *Macromolecules* **1991**, *24*, 4839.
- (5) Kambour, R. P.; Bendler, J. T.; Bopp, R. C. *Macromolecules* **1983**, *16*, 753.
- (6) ten Brinke, G.; Karasz, F. E.; MacKnight, W. J. *Macromolecules* **1983**, *16*, 1827.
- (7) Dudowicz, J.; Freed, K. F. *Macromolecules* **1997**, *30*, 5506.
- (8) Winey, K. I.; Berba, M. L.; Galvin, M. E. *Macromolecules* **1996**, *29*, 2868.
- (9) Lohse, D. J.; Graessley, W. W. Unpublished results.
- (10) Yao, S.; Kamei, E.; Matsumoto, T. *Comput. Theor. Polym. Sci.* **1997**, *7*, 25.
- (11) Balazs, A. C.; Sanchez, I. R.; Epstein, I. R.; Karasz, F. E.; MacKnight, W. J. *Macromolecules* **1985**, *18*, 2188.
- (12) Cantow, H. J.; Schulz, O. *Polym. Bull.* **1986**, *15*, 449.
- (13) Kohl, P. R.; Seifert, A. M.; Hellmann, G. P. *J. Polym. Sci., Part B* **1990**, *28*, 1309.
- (14) Bates, F. S.; Schultz, M. F.; Rosedale, J. H.; Almdal, K. *Macromolecules* **1992**, *25*, 5547. Gehlsen, M. D.; Bates, F. S. *Macromolecules* **1994**, *27*, 3611. Bates, F. S.; Fredrickson, G. H. *Macromolecules* **1994**, *27*, 1065. Fredrickson, G. H.; Liu, A. J.; Bates, F. S. *Macromolecules* **1994**, *27*, 2503. Fredrickson, G. H.; Liu, A. J. *J. Polym. Sci., Polym. Phys.* **1995**, *33*, 1203.
- (15) Krishnamoorti, R.; Graessley, W. W.; Balsara, N. P.; Lohse, D. J. *Macromolecules* **1994**, *27*, 3073. Graessley, W. W.; Krishnamoorti, R.; Balsara, N. P.; Butera, R. J.; Fetters, L. J.; Lohse, D. J.; Schulz, D. N.; Sisano, J. A. *Macromolecules* **1994**, *27*, 3896.
- (16) Graessley, W. W.; Krishnamoorti, R.; Reichart, G. C.; Balsara, N. P.; Fetters, L. J.; Lohse, D. J. *Macromolecules* **1995**, *28*, 1260.
- (17) Graessley, W. W.; Krishnamoorti, R.; Balsara, N. P.; Fetters, L. J.; Lohse, D. J.; Schulz, D. N.; Sisano, J. A. *Macromolecules* **1994**, *27*, 2574.
- (18) Schweizer, K. S.; Singh, C. *Macromolecules* **1995**, *28*, 2063. Schweizer, K. S. *Macromolecules* **1993**, *26*, 6050.
- (19) Singh, C.; Schweizer, K. S. *Macromolecules* **1997**, *30*, 1490.
- (20) Freed, K. F.; Dudowicz, J. *Macromolecules* **1996**, *29*, 625.
- (21) Dudowicz, J.; Freed, K. F. *Macromolecules* **1996**, *29*, 8960.
- (22) Krishnamoorti, R.; Graessley, W. W.; Fetters, L. J.; Garner, R. J.; Lohse, D. J. *Macromolecules* **1995**, *28*, 1252.
- (23) Freed, K. F.; Dudowicz, J.; Foreman, K. W. *J. Chem. Phys.* **1998**, *108*, 7881.
- (24) Dudowicz, J.; Freed, K. F. *Macromolecules*, submitted.
- (25) Dudowicz, J.; Freed, K. F. *Macromolecules* **1991**, *24*, 5076.
- (26) Dudowicz, J.; Freed, K. F. *Macromolecules* **1996**, *29*, 7826.
- (27) Dudowicz, J.; Freed, K. F. *Macromolecules* **1991**, *24*, 5112.
- (28) Freed, K. F.; Dudowicz, J. *Trends Polym. Sci.* **1995**, *3*, 248.
- (29) Freed, K. F.; Dudowicz, J. Unpublished results.
- (30) Russell, T. P. Private Communication; Kulasekere, R.; Kaiser, H.; Ankner, J. F.; Russell, T. P.; Brown, H. R.; Hawker, C. J.; Mayes, A. M. *Macromolecules* **1996**, *29*, 5493.
- (31) Mondello, M.; Grest, G. S.; Garcia, A. R.; Sibernagel, B. G. *J. Chem. Phys.* **1996**, *105*, 5208.
- (32) Smit, B.; Karaboni, S.; Siepmann, J. I. *J. Chem. Phys.* **1995**, *102*, 2126.
- (33) Siepmann, J. I.; Martin, M. G.; Mundy, C. J.; Klein, M. L. *Mol. Phys.* **1997**, *90*, 687. Siepmann, J. I. Private communication.
- (34) Allen, W.; Rowley, R. L. *J. Chem. Phys.* **1997**, *106*, 10273.
- (35) Reichart, G. C.; Graessley, W. W.; Register, R. A.; Krishnamoorti, R.; Lohse, D. J. *Macromolecules* **1997**, *30*, 3036.
- (36) Weimann, P. A.; Jones, T. D.; Hillmyer, M. A.; Bates, F. S.; Londono, J. D.; Melnichenko, Y.; Wignall, G. D.; Almdal, K. *Macromolecules* **1997**, *30*, 3650.
- (37) Rowlinson, J. S.; Swinton, F. L. *Liquids and Liquid Mixtures*, 3rd ed.; Butterworths: London, 1982.
- (38) Dudowicz, J.; Freed, K. F. *Macromolecules* **1995**, *28*, 6625.
- (39) Foreman, K. W.; Freed, K. F.; Ngola, I. M. *J. Chem. Phys.* **1997**, *107*, 4688.
- (40) Mc Quarrie, D. A. *Statistical Mechanics*; Harper & Row: New York, 1976.
- (41) Foreman, K. W.; Freed, K. F. *Adv. Chem. Phys.* **1998**, *103*, 335.
- (42) Foreman, K. W.; Freed, K. F. *Macromolecules* **1997**, *30*, 7295.
- (43) Dudowicz, J.; Lifschitz, M.; Freed, K. F.; Douglas, J. F. *J. Chem. Phys.* **1993**, *99*, 4804.

MA971330F